ISSN: 0975-833X

Available online at http://www.journalcra.com

International Journal of Current Research
Vol. 8, Issue, 09, pp.39537-39545, September, 2016

INTERNATIONAL JOURNAL OF CURRENT RESEARCH

RESEARCH ARTICLE

STUDY THE CORRELATION OF MUON PADDLE EFFICIENCY WITH TEMPERATURE, PRESSURE, DECOHERENCE CURVE AND EFFECT OF MULTIPLE SCATTERING PHYSICS IN GEANT4 BASED DETECTOR SIMULATION

[1]Sirisha, S. N. L., [1]Kajal Garg and [*,2]Sonali Bhatnagar

[1]Assistant Professor, Dayalbagh Educational Institute, Dayalbagh, Agra, India
[2]Department of Physics and Computer Science, Dayalbagh Educational Institute, Dayalbagh, Agra, India

ARTICLE INFO

Article History:
Received 20th June, 2016
Received in revised form
09th July, 2016
Accepted 08th August, 2016
Published online 30th September, 2016

Key words:
Total Cross-Section,
Acceptance,
Energy Loss,
Response Function,
Multiple Scattering.

ABSTRACT

The motivation behind the present study is to determine the correlation of muon count rate with the atmospheric parameters that affect the detector sensitivity. The geomagnetic cutoff rigidity i.e. 22 GeV of primary particle is computed for our muon paddle which is located at Agra, India (27.18^0 N and 78.02^0 E). The maximum solid angle of 0.15 rad is obtained for the assembly. The integral muon flux observed from analytical and experimental calculation is 9.61 / cm^2.sec.str with a statistical error of ±0.31%. The differential intensity of muon at sea level obtained from calculation is $9.12x10^{-2}$ ($sr^{-1}.cm^{-1}.sec^{-1}.$ $(GeV/c)^{-1}$). The count rate as function of detector separation (horizontal-vertical) is determined to project decoherence curve. The three fold efficiency of muon paddle ranges within (60-80)% over the period of 16 Dec 2014 – 24 Dec 2014. It marks the stability of muon detection. The correlation between temperature, atmospheric pressure and count rate was also analyzed for a duration of 1 Dec 2014 – 16 Dec 2015. The chi-square testing is also applied for the count rate where the p-value of the correlation coefficient is observed to be less than (0.01). To understand further the muon interactions and their phenomena in the detector, the muon paddle is simulated in Geant4.9.4.p04 toolkit. The effect of various surface treatments such as ground, etched and polished for each individual reflectors i.e. (Lumirror, Teflon, TiO2 and Tyvek) are also simulated to study the photon yield for incident muon. Among these reflectors, tyvek wrapping with a polished surface of dielectric_metal interface is observed to have a maximum of 96% photo yield is able to reach the sensitive region of the detector. The study further includes the multiple scattering phenomena to observe its effect on muon interactions in various density materials. The total cross-section and interaction length of muons are also computed relative to multiple scattering physics

Copyright©2016, Bhatnagar Sonali et al. *This is an open access article distributed under the Creative Commons Attribution License, which permits unrestricted use, distribution, and reproduction in any medium, provided the original work is properly cited.*

Citation: Sirisha, S.N.L., Kajal Garg and Sonali Bhatnagar, 2016. "Study the correlation of muon paddle efficiency with temperature, pressure, decoherence curve and effect of multiple scattering physics in geant4 based detector simulation", *International Journal of Current Research*, 8, (09), 39537-39545.

INTRODUCTION

Detector sensitivity for incident particle energy depends on many factors including cross-section for ionizing reactions in the detector, inherent detector noise and surface material surrounding the sensitive volume of the detector (Shubhi Parolia, 2014). The cross-section and detector mass determine the probability of the incident particle to convert its energy deposited in the detector into form of ionization. When a highly ionized charged particles incident on a detector of low density and small volume, it produces ionization resulting in a certain minimum amount of signal which is further determined by noise from the detector and its associated electronics in the form of a fluctuating voltage or current at the detector output. For a given amount of radiation type in an energy range, the total amount of ionization produced is determined by sensitive volume. A second limiting factor is the material covering the sensitive volume of the detector because of the absorption, only radiation with sufficient energy to penetrate this layer can be detected. For measurement of energy spectra, an important factor which must be considered is the response of the detector. To characterize the muon telescope, the acceptance of the detector is computed using Matlab 7.1 and its effect on varying distance among two detectors when placed in coincidence is discussed in section II. A series of calibration procedures using muon telescope were performed.

Corresponding author:** **Bhatnagar Sonali,
Assistant Professor, Dayalbagh Educational Institute, Dayalbagh, Agra, India.

The discriminator threshold and operating voltage of the photo-multiplier tube are optimized to suppress the detector noise which allows for greater sensitivity and little interference of background radiation. The significant influence of muon paddle efficiency by environmental factors like temperature and pressure are also observed. For a better understanding of the muon flux, we measured count rate dependence on varying the distance among the two muon paddles at different elevations. In section III, the muon paddle is simulated using Geant4.9.4.p04. In continuation of the work reported in the paper *S. Bhatnagar et.al. ICAM-2011, D.E.I* (Shubhangi Agarwal, 2011), the response of the telescope is observed for incident muon energy. The influence of various surfaces such as polished, etched, rough-cut surfaces for each individual reflector (Teflon tape, ESR film, Lumirror, TiO_2 paint and Tyvek paper) is observed w.r.t response of the muon telescope. The contribution to differential cross-section of the muon interaction processes in relation to the relative energy transfer function is discussed in the paper. The effect on muon interaction length and total cross-section due to multiple scattering in high and low density materials also observed.

Intensity and Energy Spectrum of Muons at Ground Level

The experiment considered for the present study mainly deals with cosmic ray muon flux using muon paddle. Initially, it is characterized for a detector setup of area 564 cm^2 (24x23.5x2 cm^3) which are placed in coincidence. The area of top detector 'A_t' defines the solid angle of acceptance 'Ω_t' for each area on 'A_b' i.e. bottom detector. It is shown in Figure 1.

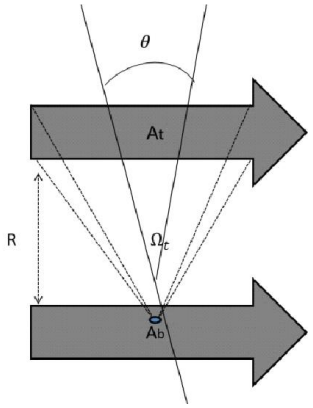

Figure 1. Geometrical description of telescope when two detectors are placed in coincidence. The dotted line shows the solid angle Ω_t subtended from top to the bottom detector and R is the distance separated

Solid angle is the acceptance of muons arriving at the detector area. For present setup, the solid angle obtained is $\Delta\Omega_2 = \frac{A_t A_b}{d^2} = 0.15\, radians$. The effect of solid angle while varying the distance between two detectors is also studied. A gradual decrease in solid angle can be observed from figure 2 on increasing the distance among the detectors. A muon at rest mass of 106 MeV/c^2 with kinetic energy of 4 GeV at sea level is considered to calculate the momentum of muon which is 920 MeV/c. the differential intensity of cosmic muons i.e. number of particles per unit area per unit time per solid angle and energy interval is also computed from muon rate for a momentum of 0.92 GeV/c which is 8.84 x 10^{-2} ($sr^{-1}.cm^{-1}.sec^{-1}.(GeV/c)^{-1}$). The correlation distance between the detectors corresponding to solid angle, count rate, integral flux and differential intensity of the muon are also studied and shown in Table 1. There is a gradual decrease in the parameter on increasing the distance. This is due to dependence of solid angle and count rate on the area of the detectors. As the distance is varied, the solid angle gets decrease which may affect the acceptance of the detector. This further leads to lesser count rate of the telescope.

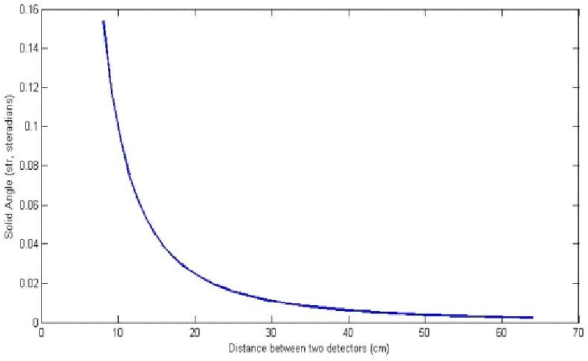

Figure 2. Effect on solid angle obtained on varying distance between two detectors when placed in coincidence

The dependency of muon differential intensity w.r.t muon momentum is also computed which is shown in table 2, where a proportional increase can be observed. The flux of cosmic ray muons is influenced by geomagnetic field is called east-west asymmetry/effect. But it is less observed at sea level due to zenith angle dependence on muon intensity. The geomagnetic cutoff rigidity provides a qualitative measure of shielding due to earth's magnetic field. It results in transmission of charged particle through magnetosphere to a specific location while following a curved path in presence of geomagnetic field and also subject to interactions with atmospheric constituents. The particles which are able to reach the earth's surface mainly depends on magnitude and direction of earth's magnetic field and also on rigidity and direction of particle propagation. The study of cosmic ray muons which are able to reach the earth's surface within geomagnetic field helps in observation of directional asymmetries detected in flux at low energies. In this paper, the cutoff rigidity (GV) of primary cosmic rays for a specified region at latitude of 28.12^0 N and longitude 78.02^0 E i.e. Agra, India where the experiment is been setup. It is calculated using stormer's equation which mainly concerns with the discrepancy between arrival directions of a particle from interplanetary space at a given location in geomagnetic field direction.

$$R_c = \frac{M\cos^4(\lambda)}{r^2[1+(1-\cos^4(\lambda)\cos(\epsilon)\sin(\zeta))^{1/2}]^2}$$

R_c is geomagnetic cutoff rigidity (in GV), M is magnitude of dipole moment in G cm^3, λ is latitude from magnetic equator, ϵ is zenith angle and ζ is azimuthal angle, r is distance from the dipole center (earth's radii). The magnitude of dipole moment has been normalized to 58 G cm^3. $R_c = \frac{14.5\cos^4(\lambda)}{r^2}$ Thus for geomagnetic latitude at 28.12^0 N with zenith angle direction in $\theta=0^0$ the obtained cut off rigidity is 22 GV. The cutoff rigidities (5) in Tsukuba (36.2^0N, 140.1^0E) and Lynn Lake (56.5^0N, 101.0^0 W) were also computed using Stormer equation, i.e. 11.4 GV and 0.4 GV respectively. The major difference among the results while comparing with present discussion is mainly due to the altitude of the experimental site considered. The angular and azimuthal dependence of cutoff rigidities is also studied at Agra, India which is located at

28.12^0 N latitude, 78.02^0 E longitude and 169 m altitude above sea level. It can be observed from figure 3. The azimuthal angle is varied from 0 to 2π direction and the cutoff rigidity of primary particle is observed for each zenith direction i.e. $0\text{-}80^0$.

detectors such as Oulu (Levin and C Moisan, 1991), ASEC (Knoll *et al*., 1998) and WILLI (Collaboration, 2012) focus on correlation studies of space and earth's atmosphere weather patterns with variation of cosmic ray neutron and muon flux.

Table 1. Correlation among the solid angle and count rate of muon telescope on varying the distance among the detectors

Vertical Separation (cm)	Solid Angle (Steradian)	Muon Rate/sec	Integral Intensity (sr^{-1}. cm^{-1}. sec^{-1})	Differential Intensity x10^{-2} (sr^{-1}. cm^{-1}. sec^{-1}. $(GeV/c)^{-1}$)	Statistical Error (%)
8	0.15	775±27	9.61	8.84	±0.31%
10	0.09	471±21	9.27	8.52	±0.41%
12	0.06	333±18	9.04	8.31	±0.53%
14	0.05	244±15	8.65	7.95	±0.54%
16	0.03	163±12	8.53	7.84	±0.60%
18	0.03	124±11	7.32	7.21	±0.65%
20	0.02	119±10	6.54	6.01	±0.68%

Table 2. Count rate obtained on varying distance among the detectors

Distance Varied	Theoretical (Muon Rate/sec)	Experimental (Muon Rate /sec)(1-12-2014 to 11-12-2014)								Error%
		Day1	Day2	Day3	Day4	Day5	Day6	Day7	Day8	
0 foot (0 m)	775	762	778	771	775	759	765	770	769	±0.01
1 foot (0.3 m)	108	98	101	95	91	97	92	96	93	±0.09
2 foot (0.7 m)	76	53	58	51	57	55	59	52	54	±0.3

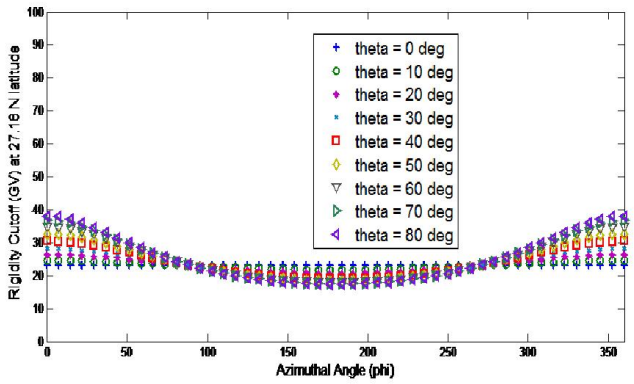

Figure 3. Effect of azimuthal angle on rigidity cutoff of primary particle w.r.t earth's surface

A significant azimuthal asymmetry is observed in the cutoff rigidity due to location which is near to the equator. The cutoff rigidity profile in different directions at different zenith angles is observed from figure. The primaries cutoff rigidity is subjected to fall at higher zenith angles. In the experimental results and discussion, two plastic scintillators embedded with WLS are used and are coupled to a PMT to amplify and convert the light to an analog signal. The setup is further associated with NIM electronics. It is used for detection of cosmic ray muons that passes through the telescope within a time interval (ns). The count rate of muons passing through two detectors comprised in the setup is 775±27/sec. the flux N is determined from observed coincidence rate $N = N_c \frac{d^2}{A_1 A_2} = 9.16 \pm 0.31/\text{cm}^2.\text{str.sec}$. It is further set to determine the efficiency and also the effect on count rate by distance separation among the detectors.

Study the muon paddle efficiency dependence on temperature and pressure

Many studies enlighten the significant role of cosmic rays in formation of low cloud coverage and its consequent impact on the global temperature variation of the earth. Ground based

The correlation of secondary cosmic ray muons flux relative to earth's atmosphere and space weather patterns was also studied by a Nuclear Physics Group of Georgia State University.

In this paper, the coincidence data of the detector is observed over a period of 16 Dec 2014 – 24 Dec 2014 to observe its effect due to temperature, pressure and humidity. The efficiency of the detector was calculated using

$$\eta = \frac{C_{D1 \cap D2 \cap D3}}{C_{D1 \cap D2}}$$

Whereη is efficiency, $C_{D1 \cap D2 \cap D3}$ is number of muons detected in D1, D2 and D3, $C_{D1 \cap D2}$is number of muons detected in D1 and D2 respectively.

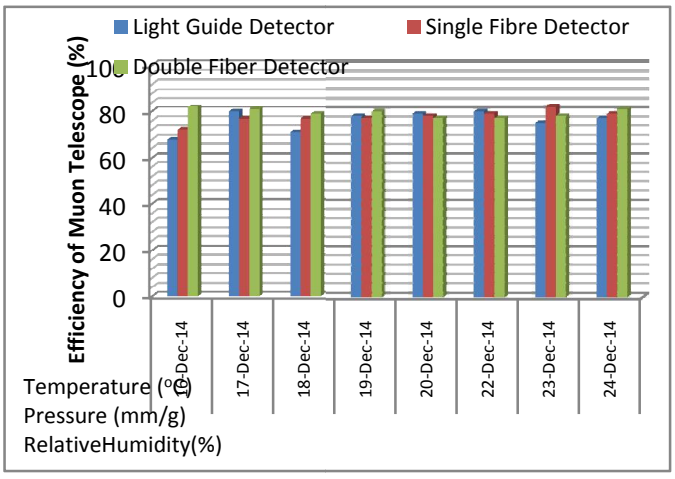

Figure 4. Efficiency of Muon Telescope as function of Temperature, Pressure and Humidity over the period from 16-December-2014 to 24-December-2014

It is observed from figure 4 that the efficiency of each detector ranges within 60 – 80 %, which also proves that telescope is suitable for muon detection.

Decoherence Curve

Measuring muon flux at different heights above the sea level is an important relativistic time dilation experiment. It is also important in many applications such as low background measurements, environmental factors like characterization of solar activity. Two plastic scintillators with fibers are considered for the present study. The count rate dependence on varying the distance between them is observed. In first case, the detectors are separated in upright and plane direction i.e. (0 foot (0 m), 1 foot (0.3 m) and 2 foot (0.7 m)) respectively. The data obtained over the period is shown in Table 2 where the count rate obtained is also compared with theoretical calculations. Here the count rate on varying the distance within the detectors is also observed at different elevations i.e. both inside a room and at roof (10m height from ground level). It is observed that the count rate gradually decreased, on increasing the distance among the detectors. But the count rate is less at ground level when compared an altitude of 10 m. Here the detector separation gives a possible approach to collect single muons and the detected coincidences are from related air shower particles. One of the most common measurements is decoherence curve, which is the rate of particle coincidences in two detectors as a function of detector separation (Knoll, 2000). Consider muons passing through a detector setup where in order to count the coincidences for a period of time. In Figure 5 (a), (b); detection results from 1 Dec. 2014 to 16 Sep. (2015) show that the count rate was relatively low at low atmospheric pressure. The motive for this outcome was absence of adjustment in the laboratory environmental temperature. Due to the variation of temperature, an expansion of change in the detection system was responsible for a direct proportional relationship between the count rate and the atmospheric pressure.

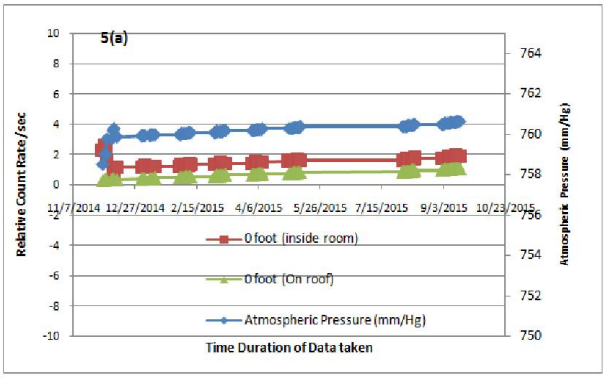

Figure 5(a): Count Rate dependence of detector coincidence as function of vertical separation among the detectors in a room

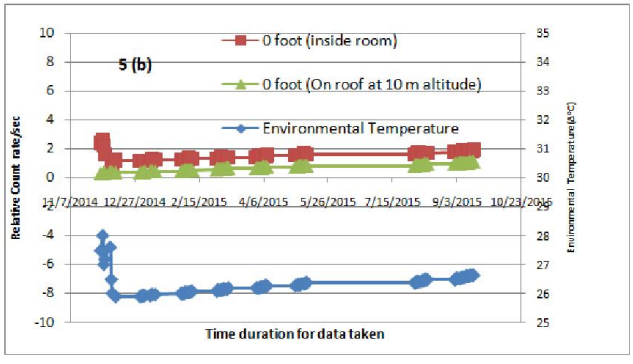

Figure 5(b): Count Rate dependence of detector coincidence as function of vertical separation among the detectors at roof (10m height from room level)

The correlation between the laboratory environmental temperature and the count rate with the chi-squared test was analyzed. The p-value for the experimental era was less than 0.01 (significance level 1%), so the correlation between the experimental temperature and the count rate was valid. The study of coincidence rate as function of detector separation helps to determine the decoherence curve. Figures 6 (a), (b); show a correlation between the count rate and the laboratory environmental temperature where it is observed that count rate is proportion to the temperature. The slope of the fitted curve also indicates the degree of dependence.

$$\frac{\Delta I}{I} = \alpha \Delta T$$

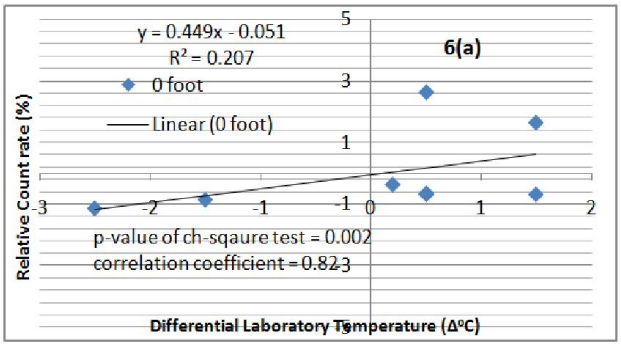

Figure 6(a): Correlation between relative coincidence rate and differential laboratory temperature

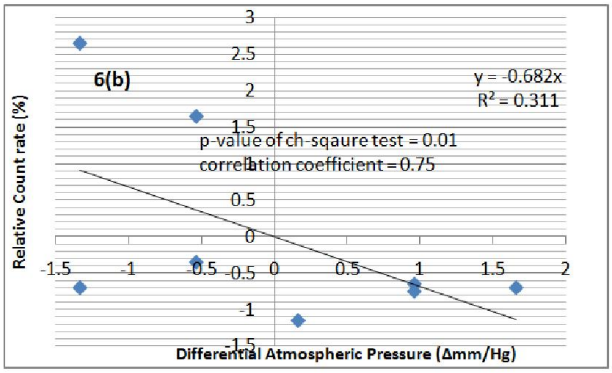

Figure 6(b): Correlation between relative coincidence rate and differential atmospheric pressure

The correlation between count rate and atmospheric pressure is also observed in inverse relation. It is due to atmosphere which acts as an absorber for muons which results in lower count rate at high pressure. Figure 6(b) also shows the response change caused by temperature correction. It is also observed to be ranging from 0.293 to -0.1112 mm/Hg. This coefficient is also influenced by cut-off rigidity because of geological factors such as latitude, longitude and altitude. It is also given from reports (20), that correlation between count rate and atmospheric pressure from 27 Sep to 5 Oct. observed ranging from -0.1% to -0.2% mm/Hg for muon detector. It is initiated by means of linear correlation between intensity and atmospheric pressure. The count rate dependence on varying the detector distance horizontally is observed along with its effect on laboratory environmental factors and is also shown in Figure 7 (a, b). It is observed that the count rate is less while compared to vertical separation due to less probability in existence of vertical slant muons while passing through both the detectors.

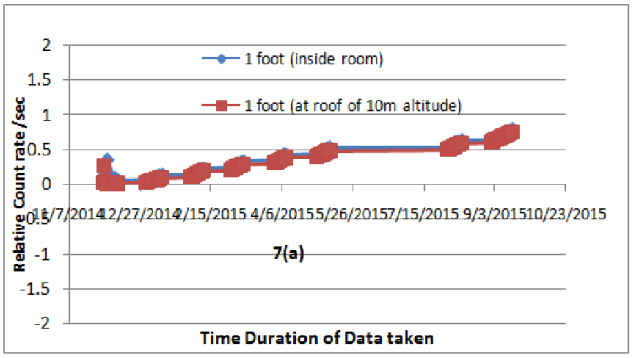

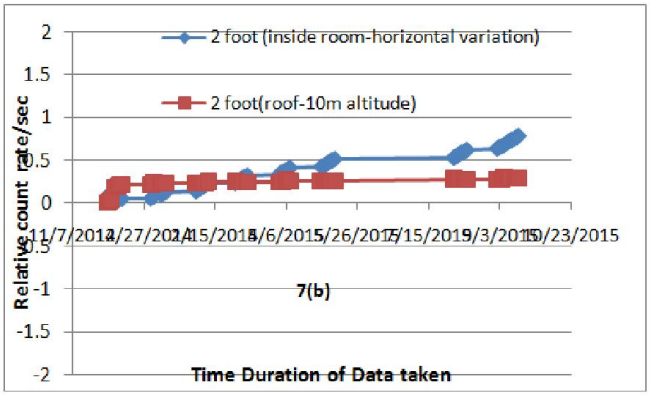

Figure 7(a, b): Count rate dependence of detector coincidence as function of horizontal separation among the detectors in a room and at roof (10m height from room level). Data taken during the period from 1-December-2014 to 16-September-2015

Geant4 simulation of Muon telescope

The muon telescope was simulated using Geant4 toolkit. The purpose of this simulation was to better understand the interaction mechanism and phenomena of multiple scattering of muons in different material densities. The entire program is executed with required modification in "TestEm17" of Geant4.9.4.p04 extended category. A plastic scintillator embedded with wave length shifting (WLS) fiber is simulated. The sensitive region of the detector is also constructed for collection of photon yield obtained from incident muon. Initially a G4RunManager is to be implemented to control the flow of the program and manages the event loops with a run. It is responsible for initialization procedure and implementing methods in user initialization classes which are defined in the form of Detector Construction and Physics List.

The detector construction comprises of three layers i.e.

G4Solid: shape/size of required geometry to be defined
G4logical volume: daughter volume where material, sensitivity, user limits are required
G4PV: Position and rotation of detector w.r.t mother volume i.e. World Volume

A box with dimensions of 24x23.5x2 cm^3 is constructed. It is assigned with material properties of different densities such as hydrogen, carbon, polystyrene and iron. Now place the detector in a coordinate system of mother volume. The bulk material propertied of polystyrene with its element composition of hydrogen and carbon were defined. Scintillation yield is one of the important optical properties of the polystyrene.

This can be adjustable using G4UImessenger class. The yield of polystyrene based plastic scintillator is 100 photon/MeV deposited energy (Saftoiu *et al*., 2011). The event generator is set for 10^6. The simulated plastic scintillator is shown in Figure 8:

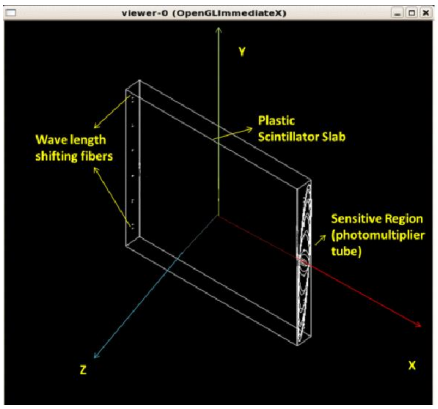

Figure 8. Plastic Scintillator designed using Geant4

The detail description of the parameters is given in paper (Shubhangi Agarwal, 2011). The characteristic light yield i.e. SCINTILLATIONYIELD, and an intrinsic resolution i.e. RESOLUTIONSCALE are defined in program which generally broadens the statistical distribution of generated photons. The relative strength of the fast component as a fraction of total scintillation yield is given by the YIELDRATIO. Scintillation is implemented by specifying these empirical parameters for each material. A relative spectral distribution as a function of photon energy for the scintillating material is defined in the Detector Construction class. The optical boundary processes are based on the concept of surface and its needs to be implemented in the form of border surface used for physical volume and skin surfaces used for logical volume of the geometry.

Model	Surfaces	Interfacing
Unified	Polished, Etched, Ground	dielectric_metal, dielectric_dielectric

There are also various surface properties along with interfacings. The UNIFIED model provides a range of different reflection mechanisms such as specular lobe constant which represents the reflection probability about the normal of a micro facet, specular spike constant that illustrates the probability of reflection about the average surface normal. A sensitive detector is implemented in G4UserSteppingAction class to count the number of photons emitted from the scintillator that hit the photocathode of the PMT. Initially the scintillator logical volume acts as a sensitive detector which yields the total energy deposited and the average position of the hit. The sensitive detector then stores the obtained values using G4VHit hits collection class. For each photon that arrives at sensitive region of PMT, the program stores the following parameters to G4UserActionClasses: the photocathode hits, number of reflections and absorptions it undergone at boundary surface of detector. The detection efficiency of the PMT photocathode is defined in terms of "quantum efficiency and "wavelength" of incident photons for a realistic case of PMT. There are also ample varieties of physics functionalities available in Geant4 "Physics List" to define the electromagnetic and hadronic processes (Mitrica, 2013).

A separate G4VPhysicsConstructor is used to define the optical physics in a module i.e. G4OpticalPhoton class. It includes the following processes: scintillation, Cerenkov, optical absorption, optical Rayleigh scattering and optical boundary processes. The muon interaction processes are simulated by implementing the necessary physics classes i.e. G4MuIonization (deals with ionization process), i.e. it provides the continuous energy loss due to ionization and simulates the discrete part of ionization i.e. delta rays produced by muons. The following models are used for the process. G4Bremstrahlung dominated the other muon interaction processes in the region of catastrophic collisions (v≥0.1) i.e. at moderate muon energies above the kinematic limit for knock-on electron production. At (E≥1TeV) this process contributes about 40% of muon energy loss. G4MuPairProduction is one of the most important processes. At TeV muon energies, the pair production cross-section exceeds over an energy transfer range 100 MeV–0.1E_{μ}. The G4MuPhotoNuclearInteraction is important at high muon energies (E≥10GeV).

Model	Energy Range
G4BraggModel	T < 0.2 MeV
G4BetherBlochModel	0.2 MeV < T < 1 GeV
G4MuBetherBlochModel	T > 1GeV

The significant energy loss of relativistic muon is independent of the energy of the muon as per the Bethe-Bloch formula (23). It is relative to the thickness of the scintillator. There is also large variation of energy loss from muon to muon which is illustrated by Landau distribution. The precise energy loss meant for any given matter and particle rate:

$$\Delta E = \xi\left[\lambda + \ln\left(\frac{5.5967.7\times10^{9}\beta^{2}}{(1-\beta^{2})Z^{2}}\xi\right)\right] + 1 - \beta^{2} - \gamma_{E}$$

$$\text{Where } \xi = \left(\frac{0.1536}{\beta^{2}}\right)\left(\frac{Z}{A}\right) S \text{ gm/cm}^{2}$$

Z and A are the atomic and mass number of material. S is the mass thickness of material and γ_E is Euler's constant = 0.577. Here a polystyrene based plastic scintillator material is considered for an influential muon energy threshold where it can start interacting with material. So, A = 104, Z = 56, S = 1.03 gm. /cm^{2}and β^2= 0.9934 for 4 GeV muon. Thus a 4 GeV muon with velocity 0.99c when passes through a polystyrene losses an energy of 2 MeV. The mean rest mass energy of muon is 105.7 MeV. In this study, the muon energy threshold is determined by considering two factors i.e. rest mass energy and mean energy loss of muon i.e. $E_{threshold}$ = 110 MeV.

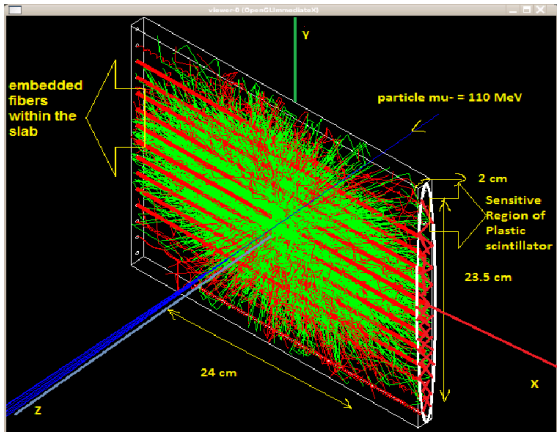

Figure 9. Response of Muon telescope for a muon of incident energy 110 MeV.

The detector simulated while muon interacting with it is shown in Figure 9. The energy deposited in detector w.r.t incident muon energy is observed as shown in figure 10 given below. The average light yield is observed to have a linear dependence on the energy deposition of muon. But this may differ in case of non-minimum ionizing particle (MIP) whereas it is vice versa in case of muon. Geant4 has different reflectors available i.e. Lumirror air, Lumirror glue, Teflon air, TiOair, Tyvek, vm2000air and vm2000 glue are implemented for polished, etched and ground surfaces with an interface of dielectric_metal and dielectric_dielectric to observe their effect on photon yield for incident muon.

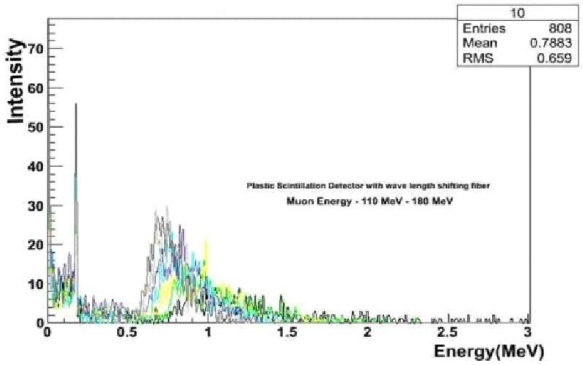

Figure 10. Plastic scintillation Detector Response for Muons from 110 MeV – 180 MeV

The simulated photon yield is displayed for polished, etched and ground surface for dielectric_dielectric and dielectric_metal interfaces in figures 11-12. Each plot corresponds to the seven reflector material attachment combinations. The parameter represents the light collected from the medium surface normalized to the light collected from the detector. The optical boundary process design is based on the concept of *surfaces* where the physical properties of the surface need to be defined a *border surface* for the relevant physical and *skin surface* for logical volumes of the geometry. There are combinations of surface finish properties, such as *polished* or *ground* and etched are available for medium boundaries (dielectric_dielectric, dielectric_metal) to study its effect on the detector response. In these conditions, the photon undergoes total internal reflection, refraction or reflection, depending on the photon's wavelength, angle of incidence, and the refractive indices on both sides of the boundary but the reflection and transmission probabilities are sensitive to the state of linear polarization. Multiple Coulomb Scattering (MCS) also leads to particle scattering and a partial role for muon energy loss. This results in increase of muon interactions corresponding to density of material. In contrast to the ionization energy loss is caused by collisions with atomic electrons. These processes are dominated by deflections in the coulomb field of nuclei. This leads to large number of scattering processes with very low deviations from original path. As a next step in this simulation study, we intended to observe the effect of multiple scattering w.r.t muon interactions in different density materials. The physics model "Wentzel VI" (25) of G4Physics List is also included along with electromagnetic interactions in present study for accurate simulation of muons and determining the energy loss in matter. This mainly helps in implementing the multiple scattering physics and also tests the scattering angle and the tangential displacement of a particle in each step. The visualization of muon interaction is viewed using HepRep Visualization Driver of Geant 4.

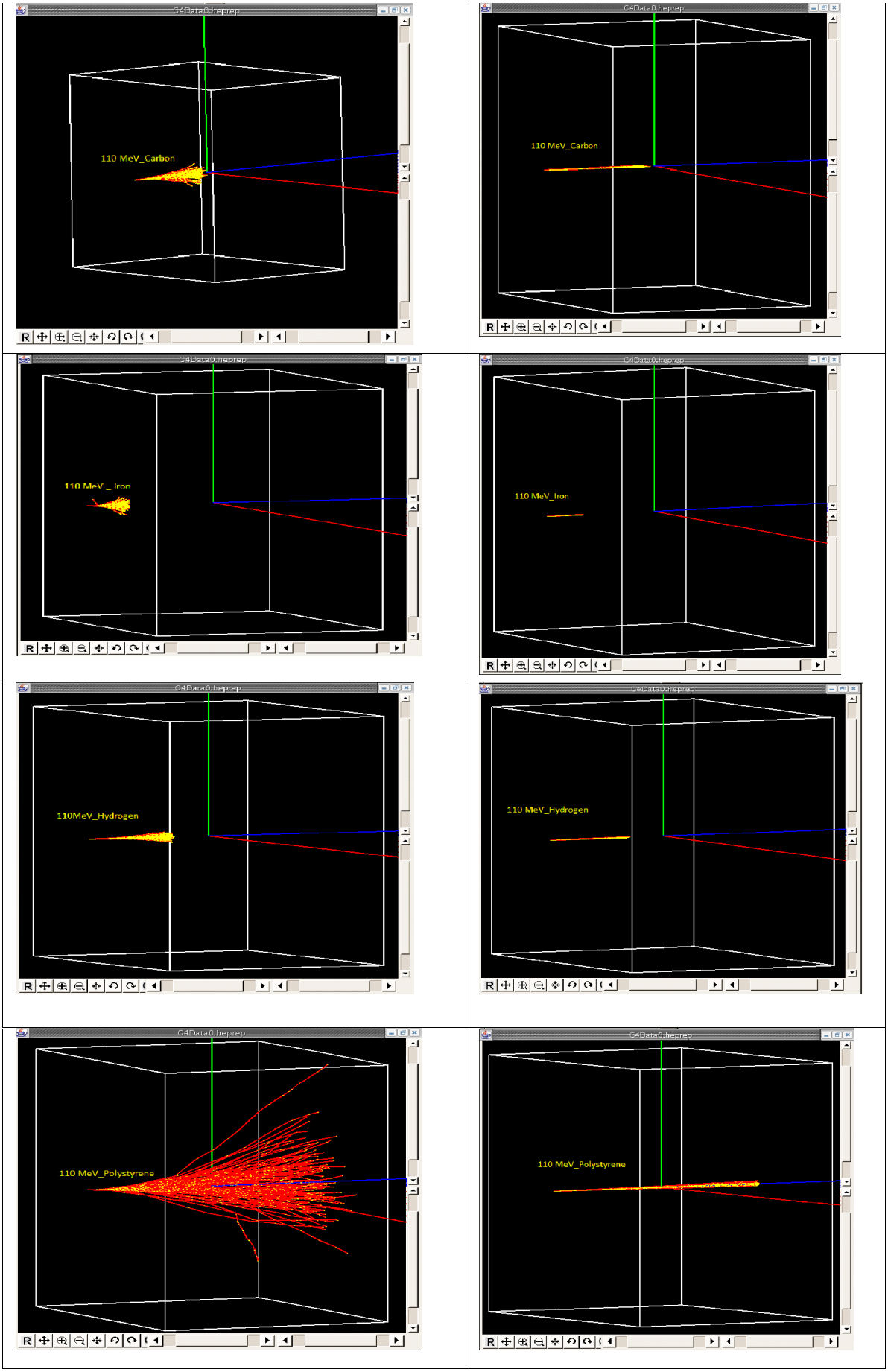

Figure 13(a-h). Visualization of Muon Interaction with different density materials on including Multiple Scattering Physics

Table 4. Effect of Multiple Scattering on Interaction Length w.r.t Muon Incident Energy

Energy (GeV)	Polystyrene		Iron		Hydrogen		Carbon	
	With Multiple Scattering	Without Multiple Scattering	With Multiple Scattering	Without Multiple Scattering	With Multiple Scattering	Without Multiple Scattering	With Multiple Scattering	Without Multiple Scattering
0.011	0.53	0.51	0.47	0.47	0.63	0.64	0.72	0.71
0.1	0.44	0.46	0.73	0.77	0.48	0.46	0.50	0.52
1.1	0.58	0.54	1.27	1.34	0.51	0.51	0.57	0.58
11	0.49	0.47	0.95	0.93	0.49	0.51	0.53	0.55

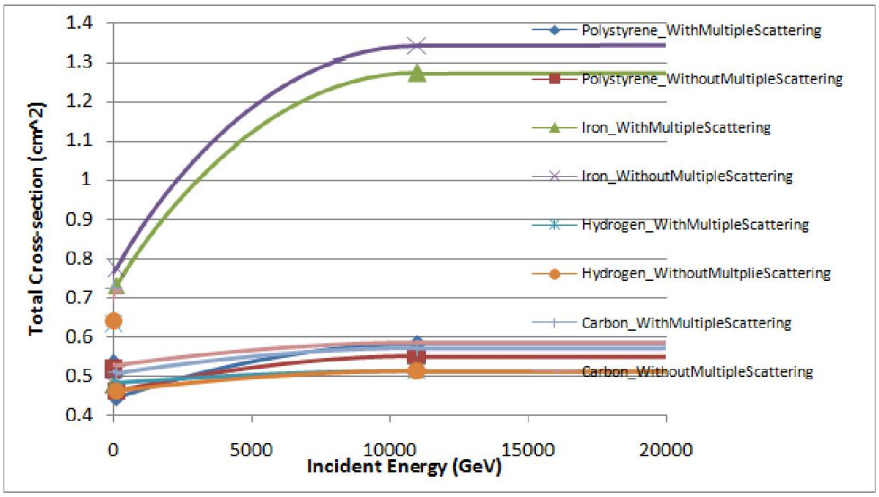

Figure 14. Effect of Multiple Scattering on Total Cross-section w.r.t Muon Incident Energy

In Figure 13(a-h) shown earlier, we can observe the muon scattering in with and without implementation of MCS physics for different material densities such as carbon, hydrogen, iron and polystyrene. The scattering of the muon in materials can be clearly seen in Figures 13 (a,c,e and g) on including multiple scattering while compared to the cases in figure 13(b,d,f and h) where the multiple scattering is not considered. The effect of MCS on total cross-section and interaction length of muon w.r.t different density material is also studied. The study is conducted by observing the dependence of total cross-section and interaction length as function of incident muon energy. This is shown in Figure 14 and Table 4. There is an exponential decrease w.r.t muon interaction length corresponding to the incident energy of muon. While total cross-section has a linear increase w.r.t energy of muon. But after a certain cut-off region of muon energy at 12E-11 eV, it is observed that both the parameters remain constant.

Conclusion

A versatile detector for cosmic ray mon flux measurements is setup and studied in this work. The concepts of scintillating, light collection and signal processing using Nuclear Instrumentation Methods (NIM) are discussed at a post graduate level by performing an educational activity. It is demonstrated by a good agreement from students feedback through a questionaire (Appendix I). The geomagnetic cutoff rigidity of primary source for particular location i.e. Agra (28.12^0 N latitude, 78.09^0 E longitude and 169 m altitude above the sea level). The effect on cutoff rigidity on varying the azimuthal ($0\text{-}360^0$) and zenith angle ($0\text{-}80^0$) is observed to be asymmetry from figure 1. The telescope is characterized on computing its solid angle and efficiency. In the present studies, for a detector area of 564 cm^2, the solid angle obtained is 0.15 radians and it is subjected to decrease exponentially from figure 3 on increasing the distance among the detectors. Further in Table 2, a correlation among muon intensity and differential energy spectrum is also computed to observe its change on varying distance among the detectors. The muon flux obtained from a coincidence rate is $9.16\pm0.31/cm^2$.str.sec. the efficiency of the telescope is further determined within 60-80%. The muon flux measurements are also computed for the setup at different altitudes on varying the distance between them. The data is taken for a duration of 1 Dec. 2014 – 16 Sep. 2015. It is also an important application for estimation of water equivalent depth for different under ground locations to characterize the back ground rate for neutrino physics like SuperKamiokanda. The application also widens in use of muon tomography technique to search the hidden rooms in pyramids or in vocabulary. There are also many applications like the detection of unknown sources to increase safety procedures such as custom check posts, scanning in vehicle transport etc. The variation of muon flux with respect to temperature, pressure and humidity possibly direct us to a new path to understand the global climate warming trend. It could also indirectly impact the solar irradiance at ground level. This may leads to catastrophic weather, crop failures, disease outbreak and impact on plants, wild life and humans. Measurement of muon flux at different heights with change of distance in detectors helps to find the primary particle source information form the obtained decoherence curve. The factors influencing the detector sensitivity such as cross-section and surrounding material of the sensitive region of muon telescope are studied. The muon interaction processes in different materials was studied in this paper using Geant4 simulation toolkit. The importance and procedure in calculation of total cross-section, interaction length and energy loss of muons was discussed. Dependance of muon cross-section mechanisms on relative energy transfer of muon to secondaries was studied. The significance of physics processes necessary for implementation

of electromagnetic interactions in Geant4 using Standard EM Package is discussed. This is done in different bulk density materials like iron, polystyrene, hydrogen and carbon. The effect of multiple scattering on muon interaction length and total cross-section within these materials is studied. The interaction length of muon is observed to have an exponential decrease in nature w.r.t energy of incident muon. While total cross-section has a linear increase w.r.t incident energy of muon. After a certain cut-off region of muon energy, both the parameters remain constant. Muon has its total cross-section relative in behavior with iron where as its interaction length is maximum for carbon. For determining the accuracy in results, step cut of incident muon is varied to observe its effect on total cross-section and interaction length. Optical photon transport is used to predict the light distribution in scintillating materials. The surface characteristics of the muon telescope based on UNIFIED optical model characterized with different properties such as specular spike, specular lobe, backscatter, and Lambertian are implemented to observe the photon yield of the plastic scintillator for polished, etched, and rough-cut surfaces. The parameter is observed for various reflectors such as Teflon tape, ESR film, Lumirror, paint, and Tyvek paper.

Acknowledgment

The authors wish to thank Cosmic Ray Laboratory (CRL), Field Station of Tata Institute of Fundamental Research, Ooty; for its technical assistance in fabricating and designing the plastic scintillation detectors. We want to express special thanks to Prof. Sunil Gupta, Shri K.C Ravindran, Shri. Atul Jain, C. Ravi and to the staff, management of Cosmic Ray Laboratory, Ooty. The authors also thank Panjab University, Inter University of Accelerator Center for their technical assistance in setting up data acquisition. We want to express special thanks to Dr. Vipin Bhatnagar, V.K Bhandari, Kundan Singh, Ruby Santhi and V.V.V Satyanarayana.

REFERENCES

Auguillar and S Beijing China. 2011. Searching for cavities in the Teotithuacan Pyramid of the Sun using cosmic muons 32nd International Cosmic Ray Conference ICRC.

Bogdanov, A.G. Burkhardt, H., Ivanchenko, V.N. Kelner, S.R. Kokoulin, R.P. Maire, *et al*. M. 2004. Geant4 Simulation of High Energy Muon Interactions. IEEE Nuclear Transactions p 7803.

Bungau. 2013. Simulation of surface muon production in graphite targets Physical reviews special topics : accelerators and beams, Vol. 16 p 147.

Cecchini. 2012. Atmospheric muons: experimental aspects Geosci. Instrum. Method Data Syst Vol. 72 p 185.

Collaboration. 2012. Geant4 User Developer, Version Geant4.9.6.p01 p 38.

Dangendorf, V. 2006. Time-resolved fast-neutron imaging with a pulse-counting image intensifier International workshop on fast neutron detectors and applications.

Geant4 Collaboration. 2012. Physics Reference manual, Version: Geant4.9.6.p01, 30th November.

Gupta, S. 2014. "High Energy Astroparticle Physics at Ooty and the GRAPES-3 Experiment", Proc Indian Natn Sci Acad , 80 No. 4, pp. 827-876.

Kim, Yun Ho. 2012. Cosmic ray measurement and experimental temperature analysis with a muon detector *Journal of Korean Physical Society* Vol. 64 p 647.

Knoll, G.F. 2000 Radiations and Measurements John Willey and Sons 3rd ed. p 281.

Knoll, G.F. Knoll, T.F. and Henderson, T.M. 1998. Light Collection Scintillation Detector COmposites for Neutron Detection. IEEE Transaction on Nuclear Sciences Vol. 35 p 181.

Levin and C Moisan. 1991. TRIUMP: A more Physical Approach to Model the Surface Treatment of Scintillation Counters and its implementation into DETECT Vol. 6 p 96.

Marteau, J., Gibert, D., Lesparre, N., Nicollin, F., Noli, P and Giacoppo, F. 2012. Muons tomography applied to geosciences and volcanology Nuclear Instruments and *Methods in Physics Research* Vol. 695 p 23.

Mitrica. 2013. A Mobile Detector for Muon Measurements based on Two Different Techniques Advances in High Energy Physics Vol. 2013 p 1.

Motoki, M., Sanuki, T., Orito, S., Abe, K. and Anraku, K *et al*. 2001. Precise Measurement of Atmospheric Muon FLux at Sea level Proceedings ICRC p 927.

O Brien and Sean, 2009. Computing the Solid Angle of Two Detectors Using Monte Carlo Methods p 15.

Ollilia A. 2012. Changes in cosmic ray fluxes improve correlation to global warming. International Journal of the Physical Sciences Vol. 822 p 35.

Peter K F. 2001. Grider Cosmic Rays At Earth 1st. ed Antony Rowe p 36.

Riggi. S. 2013. Muon tomography imaging algorithms for nuclear threat detection inside large volume containers with the Muon Portal detector. Nuclear Instruments and Methods in Physical Research A Vol. 59 p 1207.

Rubbia sl. 2010. Design Study: towards giant liquid based underground detectors for neutrino physics and astrophysics and proton decay searches Acta. Physica. Polonica B Vol. 41 p 1727.

Saftoiu, A Bercuci and I M Brancus. 2011. Measurements of the cosmic muon flux with the willi detector as a source of information about solar events Romanian Journal of Physics Vol. 56 p 664.

Shubhangi Agarwal, 2011. Study of photon yield in a plastic scintillator embedded with wave length shifting fiber. International Conference on Agile Manufacturing,, December 19-22. p - 101

Shubhi Parolia, 2014. Preliminary Studies of Muon Telescope. Advances in Radiation Measurement Systems and Techniques, March 19-21. 31st National Conference of Indian Association for Radiation Protection . pp. QR-08.

Smart, D.F. and Shea, M.A. 2005. A review of geomagnetic rigidities for earth-orbiting space craft Advances in Space Research, Vol. 36 p 2012.

****